European Spine Journal (2022) 31:1630–1639
https://doi.org/10.1007/s00586-022-07262-3

ORIGINAL ARTICLE

Adjacent segments biomechanics following lumbar fusion surgery: a musculoskeletal finite element model study

Mahdi Ebrahimkhani[1] · Navid Arjmand[1] · Aboulfazl Shirazi-Adl[2]

Received: 19 September 2021 / Revised: 18 April 2022 / Accepted: 7 May 2022 / Published online: 28 May 2022

Abstract

Purpose This study exploits a novel musculoskeletal finite element (MS-FE) spine model to evaluate the post-fusion (L4–L5) alterations in adjacent segment kinetics.

Methods Unlike the existing MS models with idealized representation of spinal joints, this model predicts stress/strain distributions in all passive tissues while organically coupled to a MS model. This generic (in terms of musculature and material properties) model uses population-based in vivo vertebral sagittal rotations, gravity loads, and an optimization algorithm to calculate muscle forces. Simulations represent individuals with an intact L4–L5, a preoperative severely degenerated L4–L5 (by reducing the disc height by ~ 60% and removing the nucleus incompressibility), and a postoperative fused L4–L5 segment with either a fixed or an altered lumbopelvic rhythm with respect to the intact condition (based on clinical observations). Changes in spine kinematics and back muscle cross-sectional areas (due to intraoperative injuries) are considered based on in vivo data while simulating three activities in upright/flexed postures.

Results Postoperative changes in some adjacent segment kinetics were found considerable (i.e., larger than 25%) that depended on the postoperative lumbopelvic kinematics and preoperative L4–L5 disc condition. Postoperative alterations in adjacent disc shear, facet/ligament forces, and annulus stresses/strains were greater (> 25%) than those found in intradiscal pressure and compression (< 25%). Kinetics of the lower (L5–S1) and upper (L3–L4) adjacent segments were altered to different degrees.

Conclusion Alterations in segmental rotations mainly affected adjacent disc shear forces, facet/ligament forces, and annulus/collagen fibers stresses/strains. An altered lumbopelvic rhythm (increased pelvis rotation) tends to mitigate some of these surgically induced changes.

Keywords Lumbar fusion surgery · Musculoskeletal finite element model · Adjacent segments · Spine loads · Kinematics

Introduction

Adjacent segment diseases (ASDs) are prevalent after lumbar fusion surgery [1]. Alterations in the kinetics of a motion segment likely paly a causal role in the mechanobiology of disc degeneration [2]. As far as postoperative ASDs are concerned, these changes may come as a result of surgically induced modifications in thoraco-lumbo-pelvic kinematics, spinal anatomy, and paraspinal muscle cross-sectional areas [3–5]. With no noninvasive in vivo technique available, in vitro setups [6] and force-controlled passive finite element (FE) models [7–9] have emerged as alternative measures to investigate the postoperative alterations in the spine biomechanics. Neglecting the crucial role of muscle forces before and after surgical interventions, however, casts doubt on the reliability of these results [10, 11]. In response, musculoskeletal (MS) models of the spine that incorporate the muscle activation have been considered when studying the effects of fusion surgery on spine kinetics [12–15].

Previous MS model studies have investigated the role of surgically induced alterations in the segmental lordosis, spinal anatomy, segmental kinematics, lumbopelvic rhythm (ratio of total lumbar rotation divided to pelvis rotation [16]), and muscle cross-sectional areas as well as the preoperative segmental conditions on the postoperative adjacent

✉ Navid Arjmand
navid.arjmand@polymtl.ca

[1] Department of Mechanical Engineering, Sharif University of Technology, Tehran 11155-9567, Iran

[2] Division of Applied Mechanics, Department of Mechanical Engineering, Polytechnique, Montréal, QC, Canada

segment kinetics [12–15]. Despite their consideration of muscle forces, these MS models nevertheless idealize passive spinal motion segments to different degrees as frictionless spherical joints, bushing elements, or shear-deformable beams with nonlinear properties. As such, they can only predict the overall segmental compression and shear loads; they fail to determine the disc compression/shear loads, ligament/facet forces, internal stresses/strains. As a remedy, hybrid models have been introduced to combine the advantages of geometrically detailed passive FE models and active musculature in MS models [17–20]. In this approach, muscle forces are first calculated using a MS model with idealized motion segments and subsequently applied in a feedforward manner onto a detailed passive FE model to determine joint load-sharing and internal stresses. This hybrid simulation, however, is cumbersome in requiring multiple rounds of analyses and corrective iterations between these two distinct models. Moreover, errors in the predicted force in muscles and passive tissues are inevitable because of the quite dissimilar passive representations in these two models and the complex load- and motion-dependent nonlinearities of the passive spine [10, 21].

Recently, we developed and validated a fully coupled MS-FE thoraco-lumbo-pelvic (T12–S1) model in which the detailed active and passive structures are both present together within a single model [21]. The present study aims to use this model to evaluate the alterations in adjacent segment kinetics following a single-level (L4–L5) solid fusion surgery. Two distinct simulations are carried out for each of the preoperative and postoperative conditions. These four simulations represent patients having: (1) an intact (healthy) or a preoperative condition with normal or mild degeneration that does not noticeably affect spinal kinematics, (2) a preoperative high-grade L4–L5 degenerated segment with substantial loss of disc height and motions, (3) a postoperative fused L4–L5 segment with fixed lumbopelvic rhythm (LPR) with respect to the intact condition (where the lost motion at the fused segment is compensated by adjacent segments) based on clinical observations [22], and (4) a postoperative fused segment with altered LPR (where the lost motion at the fused segment is compensated by the pelvis alone) based on some other observations [23]. Surgically induced changes in segmental and pelvis kinematics as well as muscle cross-sectional areas (due to intraoperative iatrogenic injuries) are considered while simulating three static daily activities. Using such a model could substantially improve our understanding of the biomechanical etiology of ASDs. It is hypothesized that different postoperative lumbopelvic (with fixed or altered rhythm) and preoperative (intact or degenerated) scenarios affect adjacent segment kinetics to quite different degrees.

Methods

Preoperative intact model

An intact preoperative L4-L5 disc condition is simulated. This represents an intact (healthy) or a preoperative condition with normal or low-grade degeneration that does not affect spinal kinematics. A previously developed coupled 3D MS-FE model consisting of the pelvis, thorax, lumbar vertebrae, intervertebral discs (nucleus and annulus as a composite of a homogeneous matrix reinforced by collagen fiber networks), ligaments, facet joints, and 56 local and global muscle fascicles with their wrapping effects is used (Fig. 1) [21]. The FE model is reconstructed in ABAQUS (version 6.12, Simulia Inc., Providence, RI, USA). For the annulus matrix, material properties are modified based on findings of a recent study [24]; a compressible Mooney–Rivlin hyperelastic model ($C_1 = 0.18$, $C_2 = 0.045$, $D = 0.2$). Annulus collagen fibers are represented with 14 distinct membrane layers reinforced with rebar elements distributed throughout the annulus matrix [10] (at $\pm 30°$ with nonlinear properties [25]). Facet joints are modeled via surface-to-surface contacts (frictionless) having a gap limit of 1.25 mm [10]. Ligaments are considered as uniaxial tension elements having nonlinear properties [25]. Each nucleus is modeled as an incompressible fluid-filled cavity [10]. The trunk weight of ~ 344 N (corresponding to a body mass of ~ 68 kg) is partitioned among upper arms (~ 36 N), forearms/hands (~ 29 N), head (46 N), and T1–L5 segments (~ 233 N) that are applied via rigid elements at their centers of mass [10]. For each activity in neutral upright standing and flexion postures ("Simulated tasks" section), the measured sagittal rotations of thorax and pelvis [26, 27] as well as the estimated individual lumbar rotations [27–29] are prescribed into the model. Sum of cubed muscle stresses was minimized through an optimization approach to determine muscle forces using an in-house code [21].

Preoperative degenerated model

A severely degenerated and narrowed L4–L5 disc is considered in the preoperative state. Fat infiltration in muscles is represented by reducing physiological cross-sectional areas (PCSAs) of paraspinal muscles; 14 and 11% for, respectively, multifidus and erector spinae at all fascicles crossing over the L4–L5 [5, 30]. The L4–L5 disc degeneration is modeled by reducing the disc height by ~ 60%, eliminating the nucleus incompressibility by setting its bulk modulus to 10 MPa, and offsetting the force–deformation curves of ligaments and fibers to account for their

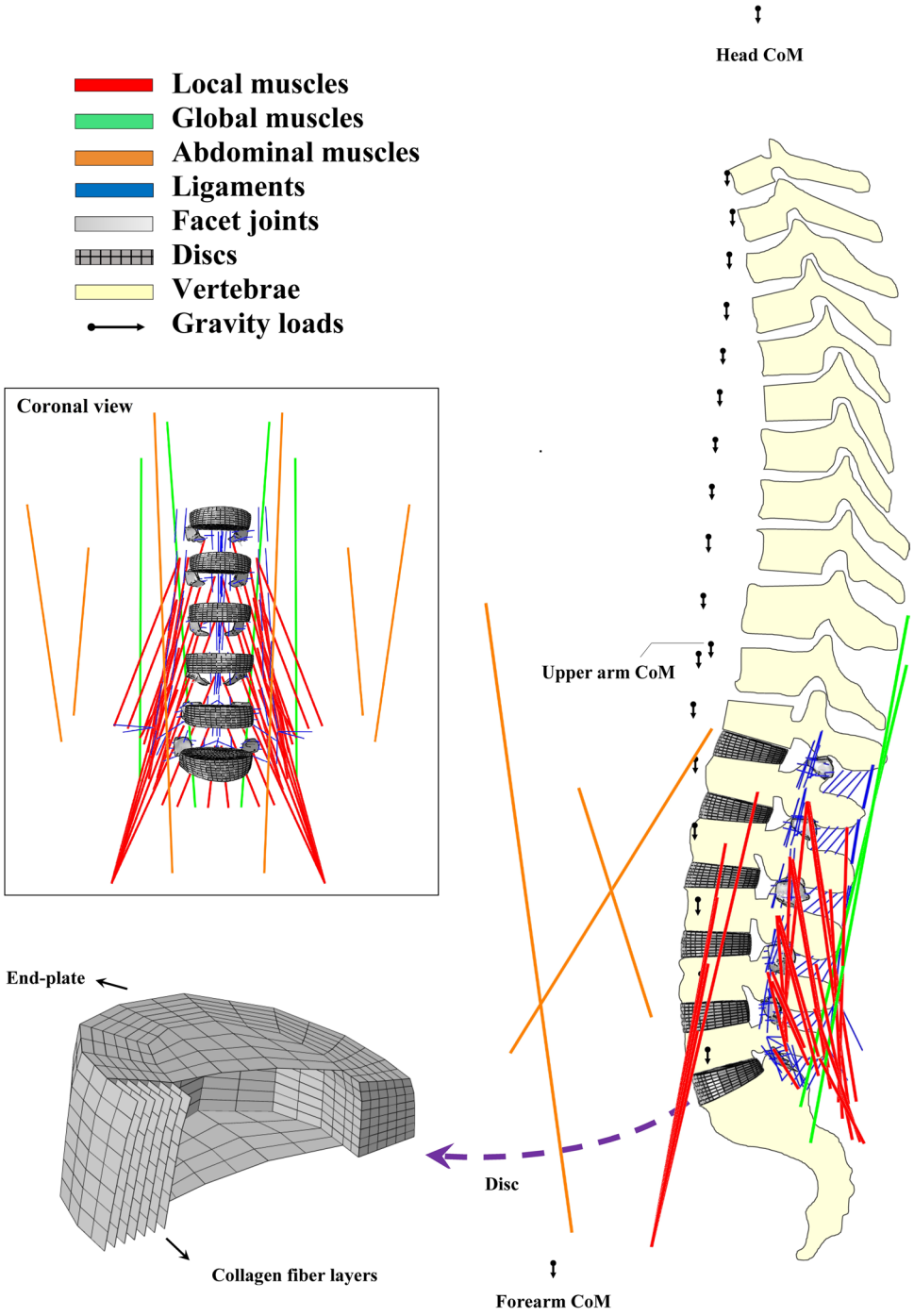

Fig. 1 The intact 3D musculoskeletal finite element (MS-FE) spine model and its musculature in the sagittal (left view) and coronal (front view) planes. Local muscles: ICPL: iliocostalis lumborum pars lumborum, LGPL: longissimus thoracis pars lumborum, MF: multifidus, QL: quadratus lumborum, and IP: iliopsoas. Global muscles: ICPT: iliocostalis lumborum pars thoracic and LGPT: longissimus thoracis pars thoracic. Abdominal muscles include: IO: internal oblique, EO: external oblique, and RA: rectus abdominis. Ligaments: the anterior longitudinal (ALL), posterior longitudinal (PLL), capsular (CL), intertransverse (ITL), ligamentum flavum (LF), supraspinous (SSL), interspinous (ISL), fascia (L4 and L5 to ilium), and iliolumbar (IL, L5 to ilium) ligaments. Vertebrae are not shown in the coronal view

slackness while preserving annulus ground material properties unchanged [31–35]. In vivo imaging data indicate that, compared to healthy individuals, LPR decreases (i.e., the contribution of the pelvis to the forward trunk flexion increases) in these patients [36, 37]. Furthermore, MR images [38] show that the loss of motion at the degenerated (i.e., stiffened) L4–L5 segment is compensated by the hypermobility of motion segments at the thoracolumbar junction. Therefore, LPR is reduced by 20% and the reduced motion at the degenerated L4–L5 segment is compensated by larger motion at the T12–L2 segments.

Postoperative fused models

Simulations of fusion are considered only for the preoperative intact model ("Preoperative intact model" section) since nearly similar postoperative models are expected for the preoperative degenerated state [12]. The fused model

has a rigidly connected L4 and L5 vertebrae. Prescribed kinematics at vertebrae and pelvis as well as injured muscle PCSAs are also as follows:

Postoperative alterations in kinematics

When the L4–L5 vertebrae are rigidly fused, the remaining segments postoperatively undergo greater rotations in order to accommodate the same posture and upper trunk flexion angle as in the preoperative condition. Based on in vivo imaging data, two approaches are adapted. First, the postoperative LPR is kept unchanged and therefore the lost L4–L5 motion is produced by the T12–L4 and L5–S1 segments. To simulate this condition, the individual lumbar rotations are recalculated based on pre- and postoperative upright X-ray measurements [22]. Second, and according to another in vivo study [23], the lost motion at the L4–L5 segment after fusion is compensated by the pelvis alone.

Alterations in muscle areas

Intraoperative injuries to paraspinal muscles are modeled based on our MR image measurements [5, 30]; the PCSAs of multifidus and erector spinae fascicles crossing over the L4–L5 segment are reduced in postoperative models by 26% and 11%, respectively.

Simulated tasks

Three regular static sagittal-symmetric daily activities in the standing are considered: one in the upright posture and two in forward trunk flexions of 40° (mid-flexion) and 80° (deep-flexion) [22, 27, 38].

Results

Changes in adjacent segment kinetics after the fusion surgery were computed that depended on the postoperative lumbopelvic kinematics and preoperative L4-L5 disc condition (Figs. 2, 3, 4, 5, 6, 7 and 8, Table 1). A substantial change (assumed here to be > 25%), as compared to the preoperative intact or degenerated states, in model outputs highlights an increase in the risk to initiate/accelerate postoperative ASDs [12]. The predicted postoperative alterations in adjacent segment gross compression and shear forces as well as global/local/total muscle forces (Figs. 2 and 3) were found, under the same load-kinematics, in overall agreement with our earlier modeling results using a MS model with segments idealized by nonlinear beams. Novel results on adjacent segment IDPs (Fig. 4), intervertebral disc compression/shear loads (Fig. 5), vector sum of all ligament/facet forces (Fig. 6), and stresses/strains in the disc (Figs. 7 and 8) that could not be predicted by the earlier MS model are therefore the focus of the present study. Postoperative alterations in adjacent level disc shear forces (Fig. 5b), facet/ligament forces (Fig. 6),

Table 1 Changes (%) in adjacent segment IDP, disc compression and shear loads, maximal annulus principal stress, posterior collagen fiber strain as well as vector sum of ligament forces and facet contact forces in fused/degenerated states relative to intact state (left section) and in fused states relative to degenerated state (right section) in upright and flexed postures. Magnitude of changes is depicted by five color-coded levels (see the legend below). Ligament forces for intact and degenerated states were ~ 0 in upright standing at both upper and lower levels and in flexion 40° at upper level. Therefore, their relative changes are depicted with (−). Note that large relative changes (%) at upper level facet forces can be seen in fused models in flexion 80° as compared to preoperative degenerated state despite the fact that their absolute changes are < 80 N (Fig. 6b)

		Compared to Intact (%)								Compared to degenerated (%)				
		Degenerated			Fused					Fused				
					Upright	Flexion (fixed LPR)		Flexion (altered LPR)		Upright	Flexion (fixed LPR)		Flexion (altered LPR)	
		Upright	Flex 40	Flex 80		Flex 40	Flex 80	Flex 40	Flex 80		Flex 40	Flex 80	Flex 40	Flex 80
Upper level	IDP	1	5	13	1	-1	-17	2	-5	0	-5	-27	-2	-16
	Disc compression	2	5	14	1	0	-9	3	-4	-1	-5	-20	-2	-15
	Disc shear	-1	-53	-25	8	9	30	-4	-11	9	130	73	102	19
	Annulus stress	-4	3	-4	3	8	27	5	0	8	5	33	2	4
	Fiber strain	1	1	-2	-1	-2	38	-2	2	-2	-3	41	-3	4
	Ligament force	-	-	-38	-	-	192	-	24	-	-	369	-	100
	Facet force	-12	-10	-81	8	-56	83	30	29	22	-51	863	44	572
Lower level	IDP	1	2	4	0	3	10	5	3	-1	0	6	2	0
	Disc compression	1	4	7	0	-4	1	3	-1	-1	-8	-6	0	-7
	Disc shear	2	6	-33	-24	-18	38	-45	-17	-26	-23	105	-48	24
	Annulus stress	0	1	2	0	9	42	6	9	0	7	39	4	6
	Fiber strain	14	3	-8	-6	34	72	3	14	-17	30	87	-1	24
	Ligament force	-	-20	-34	-	98	141	-11	0	-	147	266	11	52
	Facet force	-4	6	37	21	34	-6	59	109	24	26	-31	50	53

Large increase (%>25)	Moderate increase (10< % <25)	Negligible change (-10< % <10)	Moderate decrease (-25< % <-10)	Large decrease (%<-25)

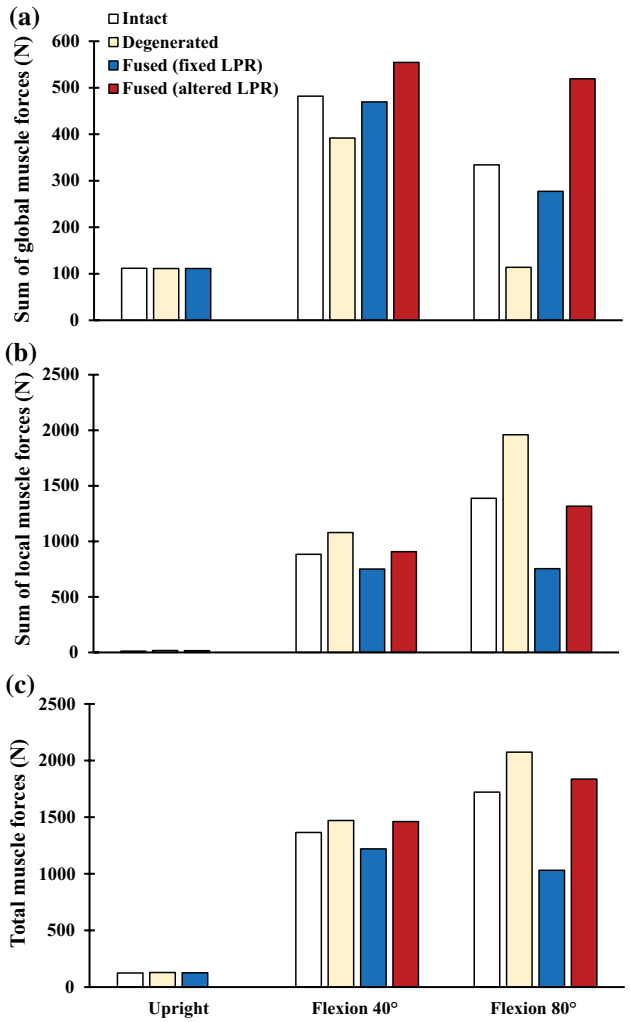

Fig. 2 Sum of bilateral forces (N) in **a** global (ICPT and LGPT), **b** local (ICPL, LGPL, IP, MF, and QL), and **c** all muscles

and annulus stresses/strains (Figs. 7 and 8) were relatively greater than those found in disc IDPs (Fig. 4) and compression forces (Fig. 5a). Adjacent segment kinetics at the lower (L5–S1) and upper (L3–L4) segments altered to different degrees following the surgery.

Degenerated versus intact models (pre-operation)

In the upright standing, predictions of the degenerated and intact models were close with changes generally negligible and < 10% (Figs. 2, 3, 4, 5, 6 and 7, Table 1). In flexion tasks, however, the degenerated model predicted overall substantially smaller global (Fig. 2a) and larger local (Fig. 2b) muscle forces, smaller disc shear forces (Fig. 5b, Table 1), smaller ligament forces (Fig. 6a, Table 1), smaller upper adjacent segment facet forces and larger lower segment facet forces (Fig. 6b, Table 1) specially at the greater flexion angle. Changes in total muscle forces (Fig. 2c), adjacent level IDPs (Fig. 4, Table 1), and disc compression forces (Fig. 5a, Table 1) were less pronounced (< 25%) in the degenerated model. Maximum principal stresses in the annulus ground substance (Figs. 7a and 8) and collagen fiber strains (Fig. 7b) remained almost unchanged with alteration generally < 10% (Table 1).

Fused model (post-operation)

In the upright standing, predictions of the fused model were generally close to those of both preoperative intact and degenerated models (Figs. 2, 3, 4, 5, 6 and 7 and Table 1). In flexion tasks with a fixed LPR, ligament forces and disc annulus stress/fiber strain substantially increased (Figs. 6, 7 and 8, Table 1). In contrast, and as a result of these increases in passive tissue load-bearing contribution, sum of total muscle forces (Fig. 2c) and, hence, segmental compression (Fig. 3a) decreased. However, alterations in adjacent disc IDPs and compression forces (Figs. 4 and 5a, Table 1) were overall less pronounced (< 25% almost everywhere). Adjacent level disc shear forces generally substantially increased especially when compared to the degenerated model (Fig. 5b and Table 1). Adjacent level facet forces were much larger at the lower level where they increased at the smaller flexion angle, whereas decreased at the larger flexion angle (Fig. 6b and Table 1).

In altered LPR models, alterations generally disappeared (Figs. 2, 3, 4, 5, 6, 7 and 8, Table 1) except for global muscle forces (Fig. 2a) and facet forces compared to both preoperative states (Fig. 6b, Table 1), disc shear forces at upper level compared to the preoperative degenerated state (Fig. 5b, Table 1), and ligament forces at large flexions as compared to preoperative degenerated state (Fig. 6a, Table 1).

Discussion

A fully coupled MS–FE spine model was used to investigate, for the first time, the effects of alterations in spinal kinematics and muscle cross-sectional areas on adjacent segment biomechanics following a single-level L4–L5 solid fusion surgery. Unlike previous passive FE models [7–9, 39, 40], this model incorporated musculature and associated distinct pre- and postoperative role of muscle activations in spinal loads. Moreover, a preoperative high-grade L4–L5 degenerated segment with substantial loss of disc height and motions was considered. Different postoperative lumbopelvic (fixed or altered lumbopelvic rhythm) and preoperative (intact or degenerated) scenarios affected adjacent segment kinetics to different degrees (hypothesis confirmed) (Table 1). Postoperative alterations in spine kinematics were found as the primary factor affecting spine biomechanics. The extent of changes is depended also on the segment (upper versus

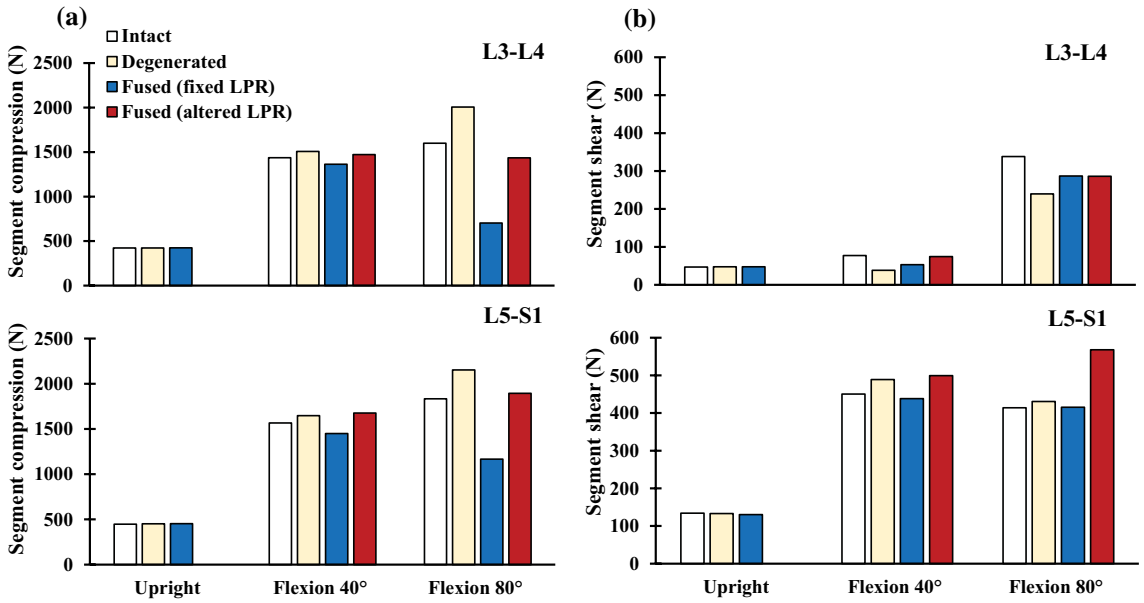

Fig. 3 Overall segmental compression (left) and shear (right) forces (N) at adjacent levels (L3–L4 and L5–S1) for different pre- and postoperative conditions in the upright and flexed postures

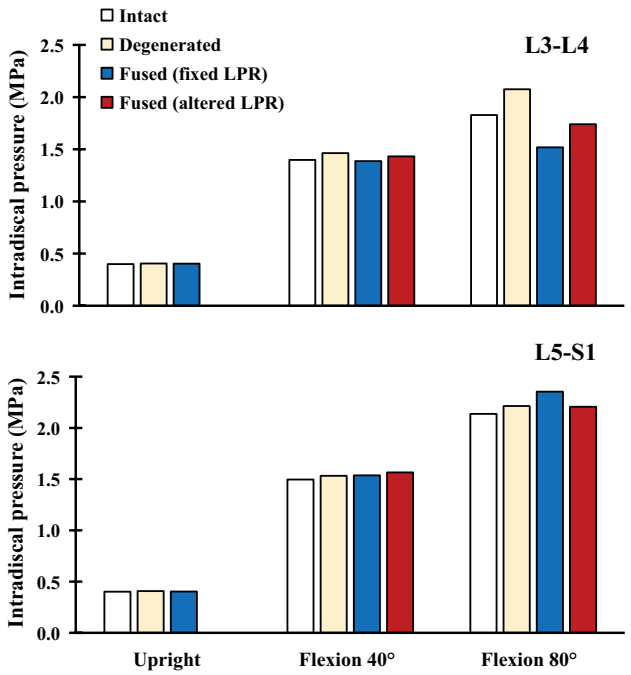

Fig. 4 Intradiscal pressure (IDP) (MPa) at adjacent levels (L3–L4 and L5–S1) for different pre- and postoperative conditions in the upright and flexed postures

lower) and preoperative condition (intact versus degenerated disc). Postoperative relative alterations in adjacent level disc shear forces (Table 1 and Fig. 5b), facet/ligament forces (Table 1 and Fig. 6), and annulus stresses/strains (Table 1, Figs. 7 and 8) were greater than those found in disc IDPs (Table 1 and Fig. 4) and disc compression forces (Table 1 and Fig. 5a). Such large changes likely play a role in the biomechanical etiology of ASDs.

Previous in silico biomechanical studies frequently considered passive FE models under idealized constant moments and compressive follower loads that remained identical in both pre- and postoperative conditions [7–9, 39, 40]. Foregoing loads actually resemble those in in vitro loading protocols rather than physiological in vivo tasks. Based on the loading protocol considered in these passive FE models (i.e., stiffness, flexibility, hybrid loading), adjacent segment IDPs and disc annulus stresses were found to either increase or remain unchanged. Segmental shear, disc shear, facet forces as well as their postoperative alterations could not accurately be predicted given the idealized nature of the compressive follower load applied [12]. In contrast, our current coupled MS-FE model simulations highlight the importance of postoperative alterations in adjacent segment shear forces that also affect facet contact loads. In accordance, clinical studies have identified listhesis and facet hypertrophy as some of the main causes of ASDs [41, 42]. Postoperative alterations in the disc compression and IDP were found less pronounced in our MS-FE model (Table 1).

Due to larger rotations at adjacent segments, forces in deeper posterior ligaments (ISL and SSL) were predicted to be much larger in the simulated fused model with fixed LPR. Fusion surgery also increased the collagen fiber strains and annulus matrix stresses (Table 1). These changes could contribute to the degradation and failure of soft tissues that

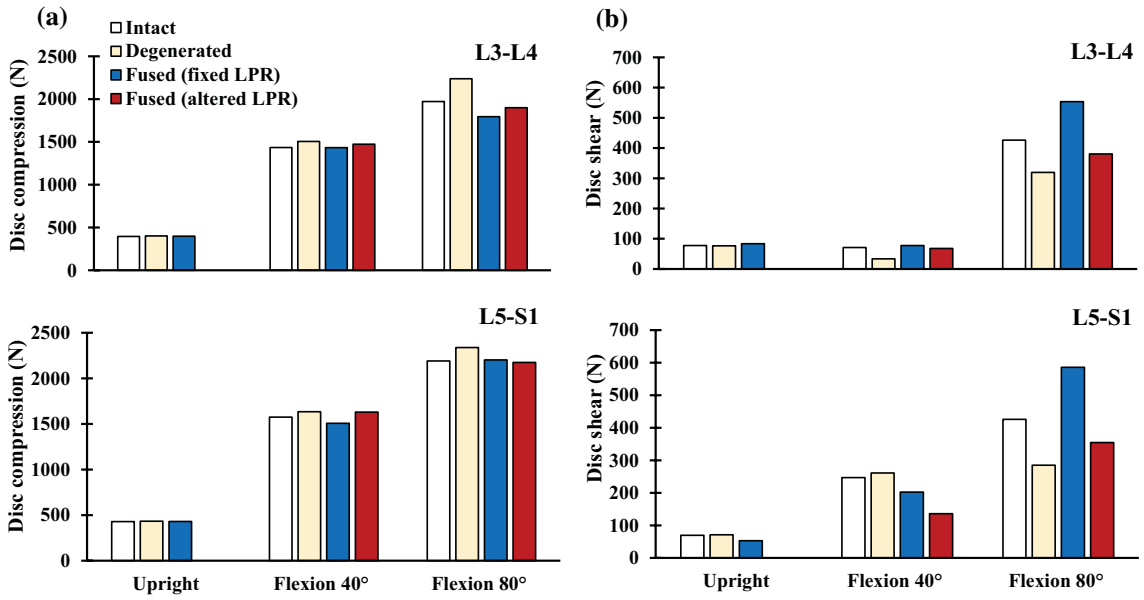

Fig. 5 Disc compression (left) and shear (right) forces (N) at adjacent levels (L3–L4 and L5–S1) for different pre- and postoperative conditions in the upright and flexed postures

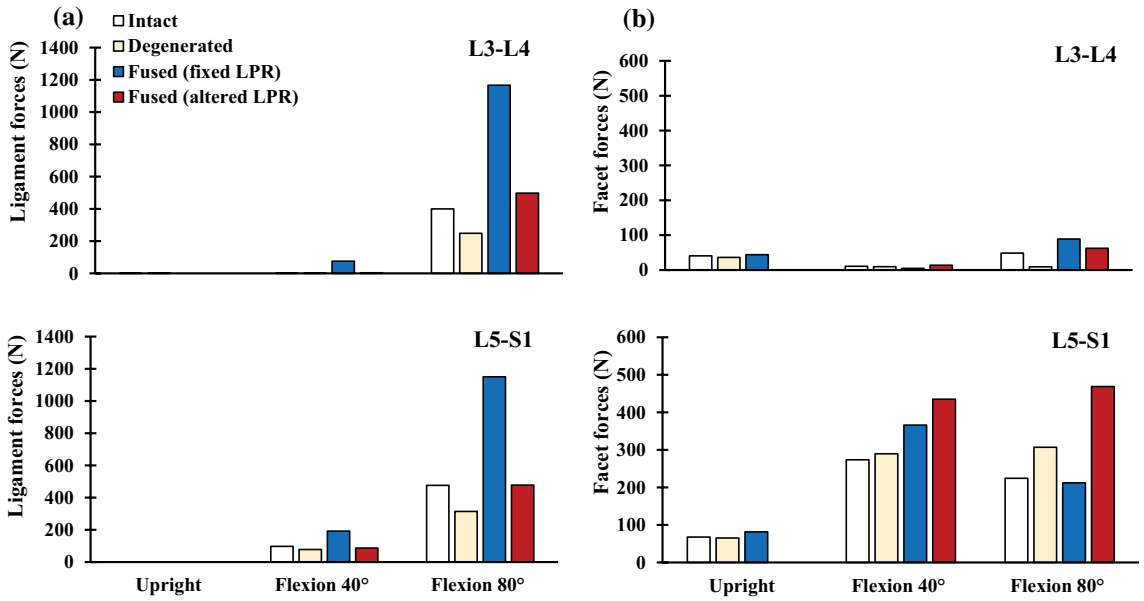

Fig. 6 Vector sum of forces in all ligaments (N) (left) and on bilateral facet articular surfaces (FJFs) (N) (right) at adjacent levels (L3–L4 and L5–S1) for different pre- and postoperative conditions in the upright and flexed postures

may ultimately result in proximal junctional kyphosis (PJK) [43] and disc prolapse [44]. Moreover, there was an increase in disc shear forces especially when compared to the preoperative degenerated state. Animal and in vitro studies have indicated that shear loading [45, 46] and hyperflexion [47] can cause disc degeneration. It therefore appears that, by substantial increases in internal forces, stresses, and strains, alterations in spine kinematics after a fusion surgery expose adjacent level discs, facets, and posterior ligaments to further risk of biomechanical damages and ASDs.

In the MS model with a detailed FE passive spine (i.e., the MS-FE model), some limitations are noteworthy. Simulations were not subject-specific; pre- and postoperative generic models were reconstructed based on the CT images

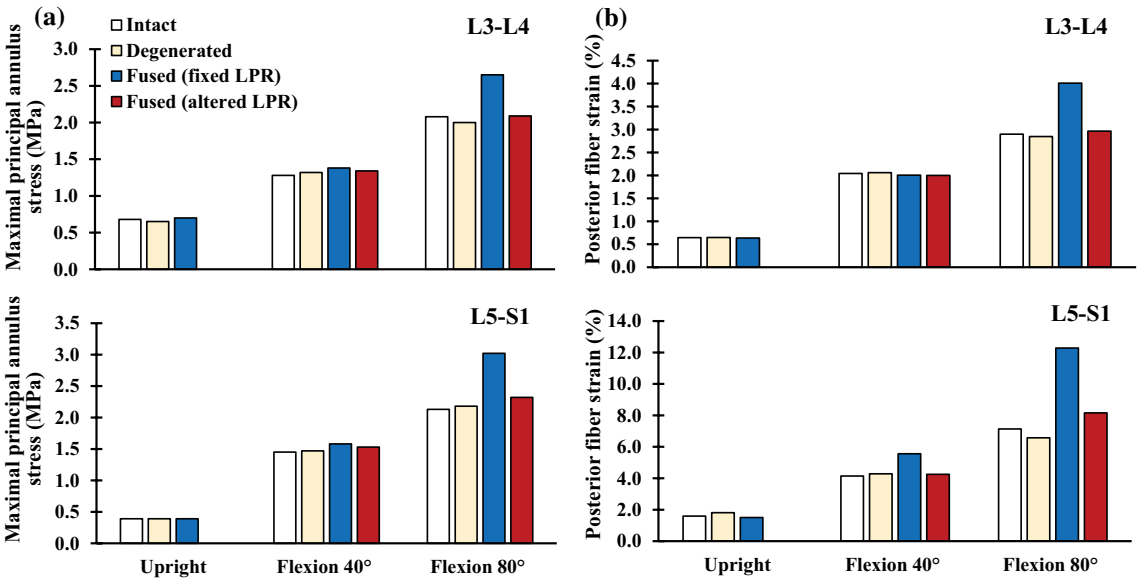

Fig. 7 Absolute maximal principal stress in the disc annulus ground substance (MPa) (left) and maximum tensile strain in the disc posterior fibers (%) (right) adjacent levels (L3–L4 and L5–S1) for different pre- and postoperative conditions in the upright and flexed postures

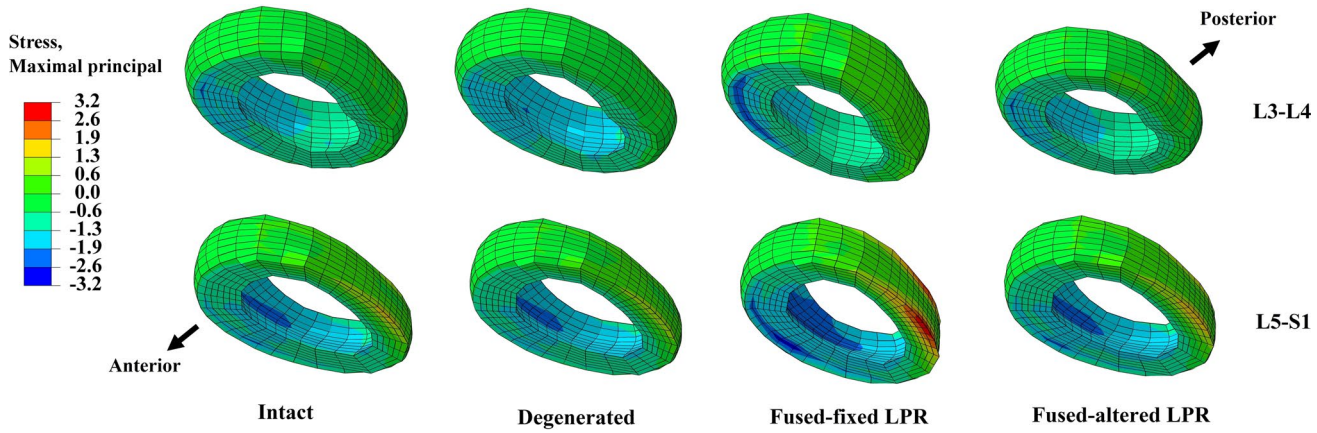

Fig. 8 Contour plots of maximal principal stresses (MPa) in the disc annulus for different pre- and postoperative conditions in the flexed posture of 80°

of a cadaver specimen [48] and driven by population-based data on the trunk musculature and passive material properties. As such and for more accurate estimations, the model should be personalized in both passive and active components [49]. Prescribed input vertebral kinematics were also based on limited population-based mean data reported in the literature. Two extreme scenarios were considered in post-fusion simulations (e.g., patients with fixed or altered postoperative lumbopelvic rhythm with respect to preoperative conditions) when compensating the eliminated motion at the fused segment while under identical trunk RoM preoperative and postoperative. Contradictory results on changes in the adjacent segment motions have been reported in the literature (e.g., increased/decreased/unchanged adjacent segment motion) [4]. However, in many of these studies, the overall trunk range of motion is not similar pre- and post-surgery. Besides, the severity of disc degeneration at the operated level could influence postoperative motions. Despite its effects on adjacent segment kinetics, available literature on changes in pelvis rotations after fusion remains limited [23]. The effects of changes in segmental lordosis or overall spinal configuration/anatomy were not considered in this study. Finally, our model employed an optimization method to estimate muscle forces; the central nervous system may adapt a different control strategy that could also differ in pre- and postoperative conditions.

Conclusion

Postoperative alterations in adjacent disc shear forces, facet/ligament forces, and annulus stresses/strains were much greater than those found in disc IDPs and compression forces. These changes that differed between the upper (L3–L4) and lower (L5-S1) adjacent segments were due primarily to postoperative alterations in lumbosacral segmental rotations. Postoperative changes in these lumbosacral angles should hence be minimized.

Acknowledgements Authors would like to appreciate the advices of Dr. Parisa Azimi on surgical procedures and the assistance of Dr. Pouria Khoddam-khorasani in FE simulations.

Funding: This work was supported by grants from Sharif University of Technology, Tehran, Iran (Grant number: G970504).

Conflict of interest The authors declare that they have no conflict of interest.

References

1. Helgeson MD, Bevevino AJ, Hilibrand AS (2013) Update on the evidence for adjacent segment degeneration and disease. Spine J 13:342–351. https://doi.org/10.1016/j.spinee.2012.12.009
2. Vergroesen PPA, Kingma I, Emanuel KS, Hoogendoorn RJW, Welting TJ, van Royen BJ, van Dieën JH, Smit TH (2015) Mechanics and biology in intervertebral disc degeneration: a vicious circle. Osteoarthritis Cartilage 23:1057–1070. https://doi.org/10.1016/j.joca.2015.03.028
3. Kumar M, Baklanov A, Chopin D (2001) Correlation between sagittal plane changes and adjacent segment degeneration following lumbar spine fusion. Eur Spine J 10:314–319. https://doi.org/10.1007/s005860000239
4. Malakoutian M, Volkheimer D, Street J, Dvorak MF, Wilke H-J, Oxland TR (2015) Do in vivo kinematic studies provide insight into adjacent segment degeneration? A qualitative systematic literature review. Eur Spine J 24:1865–1881. https://doi.org/10.1007/s00586-015-3992-0
5. Ghiasi MS, Arjmand N, Shirazi-Adl A, Farahmand F, Hashemi H, Bagheri S, Valizadeh M (2016) Cross-sectional area of human trunk paraspinal muscles before and after posterior lumbar surgery using magnetic resonance imaging. Eur Spine J 25:774–782. https://doi.org/10.1007/s00586-015-4014-y
6. Panjabi M, Malcolmson G, Teng E, Tominaga Y, Henderson G, Serhan H (2007) Hybrid testing of lumbar CHARITÉ discs versus fusions. Spine 32:959–966. https://doi.org/10.1097/01.brs.0000260792.13893.88
7. Cegoñino J, Calvo-Echenique A, Pérez-del Palomar A (2015) Influence of different fusion techniques in lumbar spine over the adjacent segments: A 3D finite element study. J Orthop Res 33:993–1000. https://doi.org/10.1002/jor.22854
8. Huang Y-P, Du C-F, Cheng C-K, Zhong Z-C, Chen X-W, Wu G, Li Z-C, Ye J-D, Lin J-H, Wang LZ (2016) Preserving posterior complex can prevent adjacent segment disease following posterior lumbar interbody fusion surgeries: a finite element analysis. PLoS ONE 11:e0166452. https://doi.org/10.1371/journal.pone.0166452
9. Srinivas GR, Kumar MN, Deb A (2017) Adjacent disc stress following floating lumbar spine fusion: a finite element study. Asian Spine J 11:538–547. https://doi.org/10.4184/asj.2017.11.4.538
10. Khoddam-Khorasani P, Arjmand N, Shirazi-Adl A (2018) Trunk hybrid passive-active musculoskeletal modeling to determine the detailed T12–S1 response under in vivo loads. Ann Biomed Eng 46:1830–1843. https://doi.org/10.1007/s10439-018-2078-7
11. Volkheimer D, Malakoutian M, Oxland TR, Wilke H-J (2015) Limitations of current in vitro test protocols for investigation of instrumented adjacent segment biomechanics: critical analysis of the literature. Eur Spine J 24:1882–1892. https://doi.org/10.1007/s00586-015-4040-9
12. Ebrahimkhani M, Arjmand N, Shirazi-Adl A (2021) Biomechanical effects of lumbar fusion surgery on adjacent segments using musculoskeletal models of the intact, degenerated and fused spine. Sci Rep 11:17892. https://doi.org/10.1038/s41598-021-97288-2
13. Ignasiak D, Peteler T, Fekete TF, Haschtmann D, Ferguson SJ (2018) The influence of spinal fusion length on proximal junction biomechanics: a parametric computational study. Eur Spine J 27:2262–2271. https://doi.org/10.1007/s00586-018-5700-3
14. Malakoutian M, Street J, Wilke H-J, Stavness I, Dvorak M, Fels S, Oxland T (2016) Role of muscle damage on loading at the level adjacent to a lumbar spine fusion: a biomechanical analysis. Eur Spine J 25:2929–2937. https://doi.org/10.1007/s00586-016-4686-y
15. Senteler M, Weisse B, Rothenfluh DA, Farshad MT, Snedeker JG (2017) Fusion angle affects intervertebral adjacent spinal segment joint forces—Model-based analysis of patient specific alignment. J Orthop Res 35:131–139. https://doi.org/10.1002/jor.23357
16. Tafazzol A, Arjmand N, Shirazi-Adl A, Parnianpour M (2014) Lumbopelvic rhythm during forward and backward sagittal trunk rotations: Combined in vivo measurement with inertial tracking device and biomechanical modeling. Clin Biomech 29:7–13. https://doi.org/10.1016/j.clinbiomech.2013.10.021
17. Honegger JD, Actis JA, Gates DH, Silverman AK, Munson AH, Petrella AJ (2021) Development of a multiscale model of the human lumbar spine for investigation of tissue loads in people with and without a transtibial amputation during sit-to-stand. Biomech Model Mechanobiol 20:339–358. https://doi.org/10.1007/s10237-020-01389-2
18. Kumaran Y, Shah A, Katragadda A, Padgaonkar A, Zavatsky J, McGuire R, Serhan H, Elgafy H, Goel VK (2021) Iatrogenic muscle damage in transforaminal lumbar interbody fusion and adjacent segment degeneration: a comparative finite element analysis of open and minimally invasive surgeries. Eur Spine J 30:2622–2630. https://doi.org/10.1007/s00586-021-06909-x
19. Khoddam-Khorasani P, Arjmand N, Shirazi-Adl A (2020) Effect of changes in the lumbar posture in lifting on trunk muscle and spinal loads: A combined in vivo, musculoskeletal, and finite element model study. J Biomech 104:109728. https://doi.org/10.1016/j.jbiomech.2020.109728
20. Liu T, Khalaf K, Adeeb S, El-Rich M (2019) Effects of lumbo-pelvic rhythm on trunk muscle forces and disc loads during forward flexion: A combined musculoskeletal and finite element simulation study. J Biomech 82:116–123. https://doi.org/10.1016/j.jbiomech.2018.10.009
21. Rajaee MA, Arjmand N, Shirazi-Adl A (2021) A novel coupled musculoskeletal finite element model of the spine – Critical evaluation of trunk models in some tasks. J Biomech 119:110331. https://doi.org/10.1016/j.jbiomech.2021.110331
22. Morishita Y, Ohta H, Naito M, Matsumoto Y, Huang G, Tatsumi M, Takemitsu Y, Kida H (2011) Kinematic evaluation of the adjacent segments after lumbar instrumented surgery: a comparison between rigid fusion and dynamic non-fusion

stabilization. Eur Spine J 20:1480–1485. https://doi.org/10.1007/s00586-011-1701-1
23. Slade CG (2018) Effects of lumbar spinal fusion on lumbopelvic rhythm during activities of daily living. University of Kentucky
24. Ghezelbash F, Shirazi-Adl A, Baghani M, Eskandari AH (2020) On the modeling of human intervertebral disc annulus fibrosus: Elastic, permanent deformation and failure responses. J Biomech 102:109463. https://doi.org/10.1016/j.jbiomech.2019.109463
25. Shirazi-Adl A, Ahmed AM, Shrivastava SC (1986) Mechanical response of a lumbar motion segment in axial torque alone and combined with compression. Spine 11:914–927. https://doi.org/10.1097/00007632-198611000-00012
26. Arjmand N, Gagnon D, Plamondon A, Shirazi-Adl A, Larivière C (2009) Comparison of trunk muscle forces and spinal loads estimated by two biomechanical models. Clin Biomech 24:533–541. https://doi.org/10.1016/j.clinbiomech.2009.05.008
27. Arjmand N, Gagnon D, Plamondon A, Shirazi-Adl A, Larivière C (2010) A comparative study of two trunk biomechanical models under symmetric and asymmetric loadings. J Biomech 43:485–491. https://doi.org/10.1016/j.jbiomech.2009.09.032
28. Dvorak J, Panjabi MM, Chang DG, Theiler R, Grob D (1991) Functional radiographic diagnosis of the lumbar spine: flexion—extension and lateral bending. Spine 16:562–571. https://doi.org/10.1097/00007632-199105000-00014
29. Frobin W, Brinckmann P, Leivseth G, Biggemann M, Reikerås O (1996) Precision measurement of segmental motion from flexion;extension radiographs of the lumbar spine. Clin Biomech 11:457–465. https://doi.org/10.1016/S0268-0033(96)00039-3
30. Jamshidnejad S, Arjmand N (2015) Variations in trunk muscle activities and spinal loads following posterior lumbar surgery: A combined in vivo and modeling investigation. Clin Biomech 30:1036–1042. https://doi.org/10.1016/j.clinbiomech.2015.09.010
31. Schmidt H, Kettler A, Rohlmann A, Claes L, Wilke H-J (2007) The risk of disc prolapses with complex loading in different degrees of disc degeneration; A finite element analysis. Clin Biomech 22:988–998. https://doi.org/10.1016/j.clinbiomech.2007.07.008
32. Rohlmann A, Zander T, Schmidt H, Wilke H-J, Bergmann G (2006) Analysis of the influence of disc degeneration on the mechanical behaviour of a lumbar motion segment using the finite element method. J Biomech 39:2484–2490. https://doi.org/10.1016/j.jbiomech.2005.07.026
33. Galbusera F, Schmidt H, Neidlinger-Wilke C, Gottschalk A, Wilke H-J (2011) The mechanical response of the lumbar spine to different combinations of disc degenerative changes investigated using randomized poroelastic finite element models. Eur Spine J 20:563–571. https://doi.org/10.1007/s00586-010-1586-4
34. O'Connell GD, Guerin HL, Elliott DM (2009) Theoretical and uniaxial experimental evaluation of human annulus fibrosus degeneration. J Biomech Eng 131:111007. https://doi.org/10.1115/1.3212104
35. Holzapfel G, Schulze-Bauer C, Feigl G, Regitnig P (2005) Single lamellar mechanics of the human lumbar anulus fibrosus. Biomech Model Mechanobiol 3:125–140. https://doi.org/10.1007/s10237-004-0053-8
36. Shojaei I, Salt EG, Bazrgari B (2020) A prospective study of lumbo-pelvic coordination in patients with non-chronic low back pain. J Biomech 102:109306. https://doi.org/10.1016/j.jbiomech.2019.07.050
37. Larivière C, Gagnon D, Loisel P (2000) The effect of load on the coordination of the trunk for subjects with and without chronic low back pain during flexion; extension and lateral bending tasks. Clin Biomech 15:407–416. https://doi.org/10.1016/S0268-0033(00)00006-1
38. Lee S-H, Daffner SD, Wang JC, Davis BC, Alanay A, Kim JS (2015) The change of whole lumbar segmental motion according to the mobility of degenerated disc in the lower lumbar spine: a kinetic MRI study. Eur Spine J 24:1893–1900. https://doi.org/10.1007/s00586-014-3277-z
39. Chen C-S, Cheng C-K, Liu C-L, Lo W-H (2001) Stress analysis of the disc adjacent to interbody fusion in lumbar spine. Med Eng Phys 23:485–493. https://doi.org/10.1016/S1350-4533(01)00076-5
40. Fan W, Guo L-X (2021) Biomechanical investigation of lumbar interbody fusion supplemented with topping-off instrumentation using different dynamic stabilization devices. Spine 46:E1311–E1319. https://doi.org/10.1097/BRS.0000000000004095
41. Lee CK (1988) Accelerated degeneration of the segment adjacent to a lumbar fusion. Spine 13:375–377. https://doi.org/10.1097/00007632-198803000-00029
42. Etebar S, Cahill DW (1999) Risk factors for adjacent-segment failure following lumbar fixation with rigid instrumentation for degenerative instability. J Neurosurg Spine 90:163–169. https://doi.org/10.3171/spi.1999.90.2.0163
43. Hostin R, McCarthy I, O'Brien M, Bess S, Line B, Boachie-Adjei O, Burton D, Gupta M, Ames C, Deviren V, Kebaish K, Shaffrey C, Wood K, Hart R, International Spine Study G (2013) Incidence, Mode, and Location of Acute Proximal Junctional Failures After Surgical Treatment of Adult Spinal Deformity. Spine 38:1008-1015. doi: https://doi.org/10.1097/BRS.0b013e318271319c
44. Shiraz-Adl A (1989) Strain in fibers of a lumbar disc: analysis of the role of lifting in producing disc prolapse. Spine 14:96–103. https://doi.org/10.1097/00007632-198901000-00019
45. Kim J, Yang S-J, Kim H, Kim Y, Park JB, DuBose C, Lim T-H (2012) Effect of shear force on intervertebral disc (IVD) degeneration: an in vivo rat study. Ann Biomed Eng 40:1996–2004. https://doi.org/10.1007/s10439-012-0570-z
46. Xia D-D, Lin S-L, Wang X-Y, Wang Y-L, Xu H-M, Zhou F, Tan J (2015) Effects of shear force on intervertebral disc: an in vivo rabbit study. Eur Spine J 24:1711–1719. https://doi.org/10.1007/s00586-015-3816-2
47. Walter BA, Korecki CL, Purmessur D, Roughley PJ, Michalek AJ, Iatridis JC (2011) Complex loading affects intervertebral disc mechanics and biology. Osteoarthritis Cartilage 19:1011–1018. https://doi.org/10.1016/j.joca.2011.04.005
48. Breau C, Shirazi-Adl A, de Guise J (1991) Reconstruction of a human ligamentous lumbar spine using CT images — A three-dimensional finite element mesh generation. Ann Biomed Eng 19:291–302. https://doi.org/10.1007/BF02584304
49. Ghezelbash F, Shirazi-Adl A, Arjmand N, El-Ouaaid Z, Plamondon A (2016) Subject-specific biomechanics of trunk: musculoskeletal scaling, internal loads and intradiscal pressure estimation. Biomech Model Mechanobiol 15:1699–1712. https://doi.org/10.1007/s10237-016-0792-3